

Supporting Information

Takahashi et al. 10.1073/pnas.0906885107

SI Text

Enhanced Green's Function Reaction Dynamics. Overview. We present the enhanced Green's Function Reaction Dynamics (eGFRD) simulation algorithm. We provide the concepts required to understand the outline of the algorithm, but details on the algorithm, such as the actual mathematical expressions for the employed Green's functions, other numerical procedures, and performance analyses, will be given in a forthcoming publication (S1).

We solve the many-body reaction-diffusion problem by decomposing it into a set of many one body (single) and two body (pair) problems, for which analytical solutions (Green's functions) exist. In the original version of the Green's Function Reaction Dynamics (GFRD) algorithm, the many-body problem was solved by determining at each step of the simulation a maximum time step Δt such that each particle could interact with at most one other particle during that time step. In practice, the maximum time step Δt was determined as follows: (1) An interaction sphere of radius $H\sqrt{6D_i\Delta t}$ is drawn around each particle, where D_i is the diffusion constant of the i -th particle, and H is a user-set error control parameter (usually 3 or 4); (2) The maximum time step Δt is then set by the requirement that each interaction sphere overlaps at most with one other interaction sphere. Subsequently, for each single particle and pair of particles a tentative reaction time is drawn, after which all particles are propagated simultaneously up to the smallest tentative reaction time, or to the maximum time step if that is smaller than the smallest tentative reaction time (S2, S3). Although already up to five orders more efficient than conventional reaction Brownian Dynamics (S4) and also very accurate by its own right, the original GFRD algorithm has three major drawbacks: (1) Because of the synchronous nature, the decomposition into one and two-body problems has to happen at every simulation step; (2) All components in the system are propagated according to the smallest tentative reaction time, making the performance sub-optimal; (3) the decomposition into single particles and pairs of particles involves cut-off distances, which makes the algorithm inexact. The systematic error is controlled by the H parameter, which determines the probability that during a time step Δt a particle travels a distance further than the maximum distance set by the requirement that each particle can interact with at most one other particle. This means that there is a trade-off between performance and error.

In the current work, we overcome the drawbacks of the original GFRD scheme by putting protective domains around single particles and pairs of particles (S5). In this scheme, the next event of a domain can either be a reaction, or one particle leaving the domain. The tentative exit time for the latter event is computed by imposing an absorbing boundary condition on the surface of the protective domain. This makes the algorithm exact, and allows for an asynchronous event-driven algorithm.

In the following sections, we explain how the reaction-diffusion problem in a spherical protective domain is solved for the one-body (Single problem) and two-body case (Pair problem), and then describe how the simulations of the different domains are integrated.

Single particle events. We consider a single particle of diameter d surrounded by a spherical protective shell of radius a (Fig. S1A). Motion of a freely diffusing spherical particle is described by the Einstein diffusion equation,

$$\partial_t p_1(\mathbf{r}, t | \mathbf{r}_0, t_0) = D \nabla^2 p_1(\mathbf{r}, t | \mathbf{r}_0, t_0), \quad [\text{S1}]$$

where the Green's function $p_1(\mathbf{r}, t | \mathbf{r}_0, t_0)$ denotes the probability that the particle is at position \mathbf{r} at time t given that it was at \mathbf{r}_0 at time t_0 . We obtain the Green's function $p_1(\mathbf{r}, t | \mathbf{r}_0, t_0)$ by solving the diffusion Eq. S1 with the following initial and boundary conditions:

$$p_1(\mathbf{r}, t_0 | \mathbf{r}_0, t_0) = \delta(\mathbf{r} - \mathbf{r}_0), \quad [\text{S2}]$$

$$p_1(|\mathbf{r} - \mathbf{r}_0| = a, t | \mathbf{r}_0, t_0) = 0, \quad [\text{S3}]$$

where δ denotes the Dirac delta function.

From the Green's function one can obtain the survival probability

$$S_1(t | \mathbf{r}_0, t_0) = \int_{|\mathbf{r} - \mathbf{r}_0| < a} d\mathbf{r} p_1(\mathbf{r}, t | \mathbf{r}_0, t_0), \quad [\text{S4}]$$

which is the probability at time t that the particle remains within the protective sphere of radius a . This is related to the probability per unit time that the particle escapes the domain for the first time,

$$q_1^{\text{escape}}(t | \mathbf{r}_0, t_0) = -\partial S(t | \mathbf{r}_0, t_0) / \partial t. \quad [\text{S5}]$$

Sampling from this escape-propensity function yields a tentative escape time t_{escape} .

It is also possible that the particle undergoes a unimolecular reaction. The probability that the next reaction happens in an infinitesimal time interval t and $t + dt$ is (S6)

$$q_1^{\text{reaction}}(t | t_0) dt = k \exp(-k(t - t_0)) dt, \quad [\text{S6}]$$

where k is the first-order reaction rate. This distribution can be used to obtain the next tentative reaction time t_{reaction} .

The next event time of a single is given by the smallest of the two tentative event times, namely,

$$t_{\text{single}} = \min(t_{\text{escape}}, t_{\text{reaction}}). \quad [\text{S7}]$$

Particle pair events. To describe the diffusion and the reaction of a pair of particles, we use the distribution function $p_2(\mathbf{r}_A, \mathbf{r}_B, t | \mathbf{r}_{A0}, \mathbf{r}_{B0}, t_0)$, which gives the probability that the particles A and B are at positions \mathbf{r}_A and \mathbf{r}_B at time t , given that they were at \mathbf{r}_{A0} and \mathbf{r}_{B0} at time t_0 . This distribution function satisfies for $|\mathbf{r}| \geq \sigma$, where $\sigma = (d_A + d_B)/2$ is the cross-section with d_A and d_B the diameters of particles A and B , respectively, the following diffusion equation:

$$\partial_t p_2(\mathbf{r}_A, \mathbf{r}_B, t | \mathbf{r}_{A0}, \mathbf{r}_{B0}, t_0) = [D_A \nabla_A^2 + D_B \nabla_B^2] p_2(\mathbf{r}_A, \mathbf{r}_B, t | \mathbf{r}_{A0}, \mathbf{r}_{B0}, t_0). \quad [\text{S8}]$$

We aim to solve this equation for two particles that can react with each other and diffuse within a protective domain. To our knowledge, it is impossible to solve this equation and obtain the Green's function directly. We therefore apply the following tricks.

First, we make a coordinate transformation

$$\mathbf{R} \equiv \frac{D_B \mathbf{r}_A + D_A \mathbf{r}_B}{D_A + D_B}, \quad [\text{S9}]$$

$$\mathbf{r} \equiv \mathbf{r}_B - \mathbf{r}_A, \quad [\text{S10}]$$

and define the operators

$$\nabla_{\mathbf{R}} \equiv \partial/\partial\mathbf{R}, \quad [\text{S11}]$$

$$\nabla_{\mathbf{r}} \equiv \partial/\partial\mathbf{r}. \quad [\text{S12}]$$

Eq. S8 can then be rewritten as

$$\partial_t p_2(\mathbf{R}, \mathbf{r}, t | \mathbf{R}_0, \mathbf{r}_0, t_0) = [D_R \nabla_{\mathbf{R}}^2 + D_r \nabla_{\mathbf{r}}^2] p_2(\mathbf{R}, \mathbf{r}, t | \mathbf{R}_0, \mathbf{r}_0, t_0), \quad [\text{S13}]$$

where $D_R \equiv D_A D_B / (D_A + D_B)$ and $D_r \equiv D_A + D_B$. This equation describes two independent random processes, one for the inter-particle vector \mathbf{r} and another for the center-of-mass vector \mathbf{R} . This means that the distribution function $p_2(\mathbf{r}_A, \mathbf{r}_B, t | \mathbf{r}_{A0}, \mathbf{r}_{B0}, t_0)$ can be factorized as $p_2^{\mathbf{R}}(\mathbf{R}, t | \mathbf{R}_0, t_0) p_2^{\mathbf{r}}(\mathbf{r}, t | \mathbf{r}_0, t_0)$ and that the above equation can be reduced to one diffusion equation for the coordinate \mathbf{R} and another for the coordinate \mathbf{r} :

$$\partial_t p_2^{\mathbf{R}}(\mathbf{R}, t | \mathbf{R}_0, t_0) = D_R \nabla_{\mathbf{R}}^2 p_2^{\mathbf{R}}(\mathbf{R}, t | \mathbf{R}_0, t_0), \quad [\text{S14}]$$

$$\partial_t p_2^{\mathbf{r}}(\mathbf{r}, t | \mathbf{r}_0, t_0) = D_r \nabla_{\mathbf{r}}^2 p_2^{\mathbf{r}}(\mathbf{r}, t | \mathbf{r}_0, t_0). \quad [\text{S15}]$$

The crux is now to define one protective domain for the inter-particle vector \mathbf{r} , with radius a_r , and another for the center-of-mass vector \mathbf{R} , with radius a_R (see Fig. S1B). These domains have to be chosen such that when the inter-particle vector \mathbf{r} and the center-of-mass vector \mathbf{R} would reach their maximum lengths, given by $|\mathbf{r}| = a_r$ and $|\mathbf{R}| = a_R$, respectively, the particles A and B would still be within the protective domain for the two particles.

The diffusion equation for the center-of-mass vector now has to be solved with the boundary conditions

$$p_2^{\mathbf{R}}(\mathbf{R}, t_0 | \mathbf{R}_0, t_0) = \delta(\mathbf{R} - \mathbf{R}_0), \quad [\text{S16}]$$

$$p_2^{\mathbf{R}}(|\mathbf{R} - \mathbf{R}_0| = a_R, t | \mathbf{R}_0, t_0) = 0. \quad [\text{S17}]$$

This problem, of the center-of-mass diffusing in its protective domain, is similar to that of the single particle diffusing in a protective domain as discussed in the previous section. From the corresponding propensity function $q_2^{\mathbf{R}}(t | \mathbf{r}_0)$ we can draw a tentative time t_R at which the center-of-mass leaves its protective domain.

The solution for the diffusion equation for the inter-particle vector is less trivial, since it should take into account not only that the inter-particle vector can leave its protective domain, but also that the two particles can react with each other. This reaction is included as an extra boundary condition, yielding the following boundary conditions for the inter-particle vector \mathbf{r} :

$$p_2^{\mathbf{r}}(\mathbf{r}, t_0 | \mathbf{r}_0, t_0) = \delta(\mathbf{r} - \mathbf{r}_0), \quad [\text{S18}]$$

$$p_2^{\mathbf{r}}(|\mathbf{r}| = a_r, t | \mathbf{r}_0, t_0) = 0, \quad [\text{S19}]$$

$$-j(\sigma, t | \mathbf{r}_0, t_0) \equiv 4\pi\sigma^2 D_r \frac{\partial}{\partial r} p_2^{\mathbf{r}}(\mathbf{r}, t | \mathbf{r}_0, t_0) |_{r=\sigma} = k_a p_2^{\mathbf{r}}(|\mathbf{r}| = \sigma, t | \mathbf{r}_0, t_0), \quad [\text{S20}]$$

where $\partial/\partial r$ denotes a derivative with respect to the inter-particle separation r . Eq. S20 is the boundary condition that describes the possibility that A and B can react with a rate k_a once they are in contact. Here, $j(\sigma, t | \mathbf{r}_0, t_0)$ is the radial flux of probability $p_2^{\mathbf{r}}(\mathbf{r}, t | \mathbf{r}_0, t_0)$ through the “contact” surface of area $4\pi\sigma^2$. This boundary condition, also known as a radiation boundary condition (S7), states that this radial flux of probability equals the intrinsic rate constant k_a times the probability that the par-

ticles A and B are in contact. In the limit $k_a \rightarrow \infty$, the radiation boundary condition reduces to an absorbing boundary condition $p_2^{\mathbf{r}}(|\mathbf{r}| = \sigma, t | \mathbf{r}_0, t_0) = 0$, while in the limit $k_a \rightarrow 0$ the radiation boundary condition reduces to a reflecting boundary condition.

From the Green’s function for the inter-particle vector \mathbf{r} , $p_2^{\mathbf{r}}(\mathbf{r}, t | \mathbf{r}_0, t_0)$, we can obtain two important quantities. The first is the time t_{bimo} at which the inter-particle vector crosses the reaction surface given by $|\mathbf{r}| = \sigma$ —meaning that the particles A and B react with each other—and the other is the time t_r at which it “escapes” through the boundary of the protective domain given by $|\mathbf{r}| = a_r$. The time at which the next event happens, be it a reaction or an escape, can be obtained through the survival probability, which is given by

$$S_2^{\mathbf{r}}(t | \mathbf{r}_0, t_0) = \int_{\sigma \leq |\mathbf{r}| < a_r} d\mathbf{r} p_2^{\mathbf{r}}(\mathbf{r}, t | \mathbf{r}_0, t_0). \quad [\text{S21}]$$

The propensity function $q_2^{\mathbf{r}}(t | \mathbf{r}_0, t_0)$, which is the probability that the next event happens between time t and $t + dt$, is related to the survival probability by

$$q_2^{\mathbf{r}}(t | \mathbf{r}_0, t_0) \equiv -\frac{\partial S_2^{\mathbf{r}}(t | \mathbf{r}_0, t_0)}{\partial t}. \quad [\text{S22}]$$

To know which of the two event types, reaction or escape, happens at time t , we split this quantity into two components,

$$q_2^{\mathbf{r}}(t | \mathbf{r}_0, t_0) = q_2^{\sigma}(t | \mathbf{r}_0, t_0) + q_2^{a_r}(t | \mathbf{r}_0, t_0) \quad [\text{S23}]$$

$$= \int_{|\mathbf{r}|=\sigma} dS D_r \frac{\partial}{\partial r} p_2^{\mathbf{r}}(\mathbf{r}, t | \mathbf{r}_0, t_0) - \int_{|\mathbf{r}|=a_r} dS D_r \frac{\partial}{\partial r} p_2^{\mathbf{r}}(\mathbf{r}, t | \mathbf{r}_0, t_0), \quad [\text{S24}]$$

where in the first term dS denotes an integral over the reaction surface at $|\mathbf{r}| = \sigma$, and in the second term an integral over the boundary of the protective domain $|\mathbf{r}| = a_r$. The reaction rate $q_2^{\sigma}(t | \mathbf{r}_0, t_0)$ is the probability that the *next* reaction for a pair of particles, initially separated by \mathbf{r}_0 , occurs at time t , while the escape rate $q_2^{a_r}(t | \mathbf{r}_0, t_0)$ yields the probability that the inter-particle distance reaches a_r and escapes from the protective domain for the first time at time t . We can draw the tentative time t for the next event, be it an escape or a reaction event, from Eq. S22, and then determine which of the two takes place from the ratio of $q_2^{\sigma}(t | \mathbf{r}_0, t_0)$ and $q_2^{a_r}(t | \mathbf{r}_0, t_0)$ at time t . Alternatively, we can draw a tentative time for a bimolecular reaction, t_{bimo} , from $q_2^{\sigma}(t | \mathbf{r}_0, t_0)$ and a tentative time for an escape event, t_r , from $q_2^{a_r}(t | \mathbf{r}_0, t_0)$; which of the two events can occur is then the one with the smallest tentative time (see below). The function $\frac{\partial}{\partial r} p_2^{\mathbf{r}}(\mathbf{r}, t | \mathbf{r}_0, t_0)$ can be used to sample the exit points on the relevant surfaces.

It is possible that the particles A and B do not only react with each other, but also can undergo a unimolecular reaction of the type $X \rightarrow \dots$. In the same way as in the Single problem (Eq. S6), we can also draw the times $t_{\text{mono},A}$ and $t_{\text{mono},B}$ at which the particles A and B undergo a first-order reaction, respectively.

The next event of a pair of particles in a protective domain is thus one of the following events: (1) the center-of-mass leaving its domain, (2) the inter-particle event leaving its domain, (3) a bimolecular reaction, (4) unimolecular reaction of molecule A , (5) a unimolecular reaction of molecule B . The event that actually takes place is the one with the smallest tentative time. The next event time for a protective domain with two particles is thus given by

$$t_{\text{pair}} = \min(t_R, t_r, t_{\text{bimo}}, t_{\text{mono},A}, t_{\text{mono},B}). \quad [\text{S25}]$$

Algorithm outline. The outline of the eGFRD algorithm is given by

1. *Initialize:* Reset the simulator time ($t_{\text{sim}} \leftarrow 0$). For each particle in the system, draw a spherical protective domain of appropriate size. When two particles are very close, create a Pair between them. Otherwise, create a Single object for each of the particles. Then, for each of the Single and the Pair objects, draw the next event type and the next event time according to the formulations in the previous sections, and chronologically order the events in the scheduler.
2. *Step:* Pick the next event with the smallest scheduled time t from the scheduler. Update the simulator time $t_{\text{sim}} \leftarrow t$. The next even could either be:

(a) *Single event*

- (a1) If the event is a *Single escape* event, then (i) propagate the particle to a randomly determined exit point on the surface of the protective domain; (ii) check if there are protective domains that are close to the new position of the particle; (iii) if there are, burst the neighboring domains, and propagate the particles in the burst domains to a new position, and check if the current Single particle can form a Pair with one of the neighboring particles; (iv) if a Pair is formed, discard the current Single, determine the new Pair event time (Eq. S25), and schedule the new Pair event on the scheduler; and (v) for each of the particles contained in the stepping Single or the burst domains that are not used in formation of the Pair, draw a new domain and schedule a Single event on the scheduler.
- (a2) If the event is *Single reaction* event, (i) propagate the particle to a point \mathbf{r} within the protective domain according to the single Green's function $p_1(\mathbf{r}, t_{\text{sim}} | \mathbf{r}_{\text{last}}, t_{\text{last}})$, where t_{last} is the time the single was created or the last time it stepped, and \mathbf{r}_{last} is the position of the particle at t_{last} ; (ii) execute the reaction by replacing the particle with one or more of the product particles placed next to each other; and (iii) for each of the newly created particles, draw a new protective domain and schedule a single event on the scheduler.

(b) *Pair event*

- (b1) If the event type is *Pair reaction*, meaning that the two particles in the domain react, (i) draw the new \mathbf{R} from $p_2^{\mathbf{R}}(\mathbf{R}, t_{\text{sim}} | \mathbf{R}_{\text{last}}, t_{\text{last}})$, where \mathbf{R}_{last} is the position of \mathbf{R} at t_{last} , which is the time at which the Pair was formed; (ii) remove particles A and B of the Pair from the simulator; (iii) place the product particle(s) at the new position \mathbf{R} ; (iv) draw protective domain(s) around the new particle(s), and schedule Single event(s) on the scheduler.
- (b2) If the event type is *r escape*, meaning that the interparticle vector \mathbf{r} leaves its protective domain, (i) sample the new \mathbf{R} position as above; (ii) sample the \mathbf{r} exit point from $\frac{\partial}{\partial \mathbf{r}} p_2^{\mathbf{R}}$; (iii) determine the new positions of A and B, \mathbf{r}_A and \mathbf{r}_B , by putting the \mathbf{R} as calculated in Eq. S1, and the exit point \mathbf{r} on the surface of the inter-particle protective domain as calculated in Eq. S2, into Eqs. S9 and S10; (iv) delete the Pair; (v) create a Single domain and schedule a new single event on the scheduler for both A and B.
- (b3) If the event type is \mathbf{R} *escape*, meaning that the center-of-mass leaves its domain, (i) sample the new interparticle vector \mathbf{r} with $p_2^{\mathbf{r}}(\mathbf{r}, t_{\text{sim}} | \mathbf{r}_{\text{last}}, t_{\text{last}})$, where \mathbf{r}_{last} is the interparticle vector at the time t_{last} it was last updated; (ii) sample the \mathbf{R} exit point from $\frac{\partial}{\partial \mathbf{R}} p_2^{\mathbf{R}}$; (iii) displace the particles A and B to the

new positions; (iv) delete the Pair; (v) create two Singles and schedule them on the scheduler.

- (b4) If the event type is *Single reaction*, (i) burst the pair domain and update the positions of the particles A and B by sampling $p_2^{\mathbf{R}}(\mathbf{R}, t_{\text{sim}} | \mathbf{R}_{\text{last}}, t_{\text{last}})$ and $p_2^{\mathbf{r}}(\mathbf{r}, t_{\text{sim}} | \mathbf{r}_{\text{last}}, t_{\text{last}})$; (ii) execute the reaction of the reacting particle according to the same procedures as used in the *Single* event; (iii) create a new *Single* domain for the other (non-reacting) particle and schedule it on the scheduler.

3. Go to 2.

It can happen that more than two particles come very close to each other, making it difficult to draw protective domains of sufficient size around each of the particles (S5); this could bring the simulations to a standstill. To preempt this scenario, the algorithm puts one protective domain around the “squeezed” particles to form a third type of object called “Multi.” The particles in this domain are propagated according to Brownian dynamics (S4) until the particles recover from the squeezed condition. Because it is guaranteed that Brownian dynamics converges to the correct solution when a sufficiently small step size is used (S4), this squeezing recovery procedure does not affect the overall accuracy of the simulation.

The actual forms of the single and Pair Green's functions, efficient numerical evaluation methods for the Green's functions, more details on the algorithm including the recovery procedure from squeezing, and handling of surfaces will be described in a forthcoming publication (S1).

Rebinding-time distribution. In this section we present scaling relations for the rebinding-time distributions of two particles that can diffuse and react with each other in a large compartment. These results give a mathematical interpretation of the non-monotonic form of the enzyme-substrate rebinding-time distributions, shown in Fig. 4A and B of the main text.

The problem is reduced to solving the reaction-diffusion equation for a random walker that can diffuse in a domain internally bounded by a sphere of radius σ , and to which it can bind with an intrinsic rate k_a once it is in contact with the sphere. This represents the evolution of the inter-particle vector \mathbf{r} describing the distance between a substrate molecule and the enzyme molecule that has just modified it.

The rebinding probability can be obtained from the Green's function $p_2(\mathbf{r}, t | \mathbf{r}_0, t_0)$. The probability that a particle that starts at the origin given by $|\mathbf{r}| = \sigma$ returns to the origin at a later time t , is given by

$$p_2(\sigma, t | \sigma, 0) = \frac{\sigma - e^{D t \alpha^2 / \sigma^2} \sqrt{\pi D t} \alpha \operatorname{erfc}\left(\alpha \sqrt{\frac{D t}{\sigma^2}}\right)}{4 \pi \sigma^3 \sqrt{\pi D t}}, \quad [\text{S26}]$$

where $\alpha = 1 + h\sigma$ and erfc is the complementary error function. If we assume that the enzyme becomes active immediately after enzyme-substrate dissociation, then, according to Eq. S20, the rebinding-time probability distribution can be expressed as

$$p_{\text{reb}}^0(t) = k_a p_2(\sigma, t | \sigma, 0). \quad [\text{S27}]$$

This rebinding-time distribution has a number of properties. Firstly, the total probability that there is a rebinding is smaller than one:

$$\int_0^\infty dt p_{\text{reb}}(t) = \frac{1}{1 + \frac{4\pi D \sigma}{k_a}} < 1. \quad [\text{S28}]$$

Secondly, upon a variable change $t = \tau \frac{\sigma^2}{D(1+k_a/(4\pi D \sigma))^2}$, the rebinding probability distribution can be rescaled as

$$p_{\text{reb}}(\tau) = \frac{1}{1 + \frac{4\pi D\sigma}{k_a}} f(\tau), \quad f(\tau) = \left[\frac{1}{\sqrt{\pi\tau}} - e^\tau \text{erfc}(\sqrt{\tau}) \right]. \quad [\text{S29}]$$

The function $f(\tau)$ has the shape of two power laws $f(\tau) \simeq \frac{1}{\sqrt{\tau}}$ for $\tau \ll 1$ and $f(\tau) \simeq \frac{1}{\tau\sqrt{\tau}}$ for $\tau \gg 1$, in accordance with the results presented in Figure 2 of the main text. In fact, we can estimate the time for the inflection point to be $\tau_{\text{mol}} = \frac{\sigma^2}{D(1+k_a/(4\pi D\sigma))}$. Here, τ_{mol} represents the time after which most of the rebindings correspond to particles that start at contact, but wander away from the reaction sphere before they return to and rebind the reaction sphere. We stress that these trajectories are rebinding trajectories; we thus exclude trajectories where particles diffuse in the bulk and come back in a memory-less fashion (see also below). The $t^{-1/2}$ scaling for $t < \tau_{\text{mol}}$ can be understood by noticing that on this time scale particles stay close to the surface of the reaction sphere; indeed, on this time scale the particles essentially see a flat reaction surface, meaning that the return-time distribution is that of a 1D random walker as described in the main text. The $t^{-3/2}$ scaling for $t > \tau_{\text{mol}}$ can be understood by observing that on this time scale the particles have diffused away from the surface of the sphere; the particles now see the entire sphere, which means that the rebinding-time distribution is that of a 3D random walker returning to the origin. Interestingly, τ_{mol} depends on k_a . When k_a is increased, the probability that a particle binds the target upon contact increases. Hence, the probability that after a time t the particle is still performing a 1D random walk close to the surface, decreases as k_a increases—the particle has either reacted with the surface, or escaped from the surface, thus performing a 3D random walk.

So far we have assumed that upon dissociation, the enzyme and substrate can rebind as soon as they are in contact again. If, however, they can only rebind after the enzyme has become active again, then the rebinding-time distribution is given by

$$p_{\text{reb}}(t) = \int_0^t dt' \int_\sigma^\infty 4\pi r^2 dr p_2^*(r, t'|\sigma, 0) k_a p_{\text{act}}(t') p_2(\sigma, t-t'|r, 0), \quad [\text{S30}]$$

where

$$p_{\text{act}}(t) = k_{\text{act}} e^{-k_{\text{act}} t} \quad [\text{S31}]$$

is the enzyme reactivation distribution with $k_{\text{act}} \equiv 1/\tau_{\text{rel}}$, and $p_2^*(r, t|r_0, 0)$ is the solution of the Smoluchowski equation with a reflecting boundary condition—this reflects the idea that when the enzyme has not become active yet, the substrate cannot bind it.

Whereas we do not know an analytical expression for the rebinding-time distribution of Eq. S30, we can derive a lower bound $p_{\text{reb}}^{\text{min}}(t)$ and an upper bound $p_{\text{reb}}^{\text{max}}(t)$ for it, such that $p_{\text{reb}}^{\text{min}}(t) \leq p_{\text{reb}}(t) \leq p_{\text{reb}}^{\text{max}}(t)$. The upper bound $p_{\text{reb}}^{\text{max}}(t)$ is based on the inequality

$$p_2(\sigma, t-t'|r, 0) \leq p_2(\sigma, t-t'|\sigma, 0), \quad [\text{S32}]$$

with equality for $r = \sigma$. This inequality expresses the fact that the probability that the particles are in contact at a later time t decreases with the initial distance. This yields the upper bound

$$p_{\text{reb}}^{\text{max}}(t) = \int_0^t dt' k_a p_{\text{act}}(t') p_2(\sigma, t-t'|\sigma, 0). \quad [\text{S33}]$$

Using the solution for $p_2(\sigma, t-t'|\sigma, 0)$ as described in S29 one can show that for small t the bound increases with t as \sqrt{t} , while for large t it decreases with t as $\frac{1}{\sqrt{t}}$. The upper bound $p_{\text{reb}}^{\text{max}}(t)$ thus has a non-monotonic behavior, going to zero at both zero and

infinity. The position of the maximum depends on the two time scales $\tau_{\text{rel}} = 1/k_{\text{act}}$ and τ_{mol} and is located in the interval $[\text{MIN}(\tau_{\text{mol}}, \tau_{\text{rel}}), \text{MAX}(\tau_{\text{mol}}, \tau_{\text{rel}})]$.

The lower bound $p_{\text{reb}}^{\text{min}}(t)$ is based on the inequality $p_2(r, t|\sigma, 0) \leq p_2^*(r, t|\sigma, 0)$. This reflects the idea that with a radiation boundary condition, the particle can react with the reactive sphere (and thus leak out of the system), whereas with a reflecting boundary condition it cannot. This yields the following expression for the lower bound

$$p_{\text{reb}}^{\text{min}}(t) = \int_0^t dt' k_a p_{\text{act}}(t') p_2(\sigma, t|\sigma, 0), \quad [\text{S34}]$$

$$= (1 - e^{-k_{\text{act}} t}) k_a p_2(\sigma, t|\sigma, 0), \quad [\text{S35}]$$

$$= s_{\text{act}}(t) p_{\text{reb}}^0(t), \quad [\text{S36}]$$

where $s_{\text{act}}(t)$ is the probability that the enzyme is active after time t and $p_{\text{reb}}^0(t)$ is the enzyme-substrate rebinding-time distribution assuming that the enzyme is active at all times. This lower bound has a number of interesting scaling regimes, depending on the relative values of τ_{rel} and τ_{mol} . They can be understood intuitively by making the following observations: as discussed above, for $t < \tau_{\text{mol}}$, $p_{\text{reb}}^0(t) \sim t^{-1/2}$, while for $t > \tau_{\text{mol}}$, $p_{\text{reb}}^0(t) \sim t^{-3/2}$; moreover, for $t \ll \tau_{\text{rel}}$, $s_{\text{act}}(t) \sim t$, while for $t \gg \tau_{\text{rel}}$, $s_{\text{act}}(t) \rightarrow 1$. Hence, for $t < \text{MIN}(\tau_{\text{mol}}, \tau_{\text{rel}})$, $p_{\text{reb}}^{\text{min}}(t) \sim t^{-1/2} \times t \sim t^{1/2}$, while for $t > \text{MAX}(\tau_{\text{mol}}, \tau_{\text{rel}})$, $p_{\text{reb}}^{\text{min}}(t) \sim t^{-3/2}$. Moreover, when $\tau_{\text{rel}} < \tau_{\text{mol}}$, $p_{\text{reb}}^{\text{min}}(t) \sim t^{-1/2}$ for $\tau_{\text{rel}} < t < \tau_{\text{mol}}$, because $s_{\text{act}} \rightarrow 1$ and $p_{\text{reb}}^0(t) \sim t^{-1/2}$. And in the scenario that $\tau_{\text{mol}} < \tau_{\text{rel}}$, $p_{\text{reb}}^{\text{min}}(t) \sim t^{-1/2}$ for $\tau_{\text{mol}} < t < \tau_{\text{rel}}$, because $s_{\text{act}} \sim t$ and $p_{\text{reb}}^0(t) \sim t^{-3/2}$.

Fig. S2 shows the predictions of the upper bound Eq. S33 and lower bound Eq. S36 for the rebinding-time distribution given by Eq. S30, for three different scenarios: (1) $\tau_{\text{rel}} \ll \tau_{\text{mol}}$ (Blue line); (2) $\tau_{\text{rel}} \approx \tau_{\text{mol}}$ (Green line); (3) $\tau_{\text{rel}} > \tau_{\text{mol}}$ (Red line). It is seen that in all three scenarios the upper and lower bound for $p_{\text{reb}}(t)$ converge for $t > \tau_{\text{rel}}$. Indeed, in this regime, where the enzyme is active, $p_{\text{reb}}(t)$ scales as $t^{-3/2}$. It is also observed that when $\tau_{\text{rel}} \leq \tau_{\text{mol}}$ (Blue and Green lines), the difference between the upper and lower bound for $p_{\text{reb}}(t)$ is very small, even when $t < \tau_{\text{rel}}$. This implies that both bounds are good approximations for $p_{\text{reb}}(t)$; we can thus conclude that, to a good approximation, $p_{\text{reb}}(t)$ scales as $t^{1/2}$ for $t < \text{MIN}(\tau_{\text{rel}}, \tau_{\text{mol}})$ and $t^{-1/2}$ for $\tau_{\text{rel}} < t < \tau_{\text{mol}}$ when $\tau_{\text{rel}} < \tau_{\text{mol}}$. The difference between the bounds arises when $\tau_{\text{rel}} > \tau_{\text{mol}}$ (Red line); in this scenario, the bounds differ in the regime $\tau_{\text{mol}} < t < \tau_{\text{rel}}$. The question arises which bound is closer to the actual rebinding-time distribution, $p_{\text{reb}}(t)$. To this end, we compare our analytical results with the simulation data, shown in Fig. S3.

In Fig. S3 we show the simulation results of Fig. 4 of the main text. When $t \geq \tau_{\text{bulk}}$ the rebinding-time distribution is exponential. This is due to particles that come from the bulk, and bind the reactive sphere in a memory-less fashion. This regime is not described by the analysis discussed above, which is performed for the geometry of an infinite, spherical domain internally bounded by a reactive sphere. For this geometry, in three dimensions, there is a probability that the particle escapes to infinity without returning to and reacting with the reactive sphere. In a bounded domain, when a particle escapes from the vicinity of the reactive sphere into the bulk, it will return to the reactive sphere on a time scale τ_{bulk} . Therefore, the rebinding-time distributions for the infinite domain analyzed above and the finite domain of the simulations, are the same, but only up to τ_{bulk} . This also means that to observe the different power-law scaling behaviours, $\tau_{\text{bulk}} \gg \text{MAX}(\tau_{\text{rel}}, \tau_{\text{mol}})$.

In A of Fig. S3, $\tau_{\text{rel}} \approx \tau_{\text{mol}}$, while in panel B $\tau_{\text{rel}} \gg \tau_{\text{mol}}$. In both scenarios $p_{\text{reb}}(t) \sim (t)^{1/2}$ when $t < \text{MIN}(\tau_{\text{rel}}, \tau_{\text{mol}})$, in accordance with the analysis of the upper and lower bounds of $p_{\text{reb}}(t)$

presented above. Both panels also show that when $\text{MAX}(\tau_{\text{mol}}, \tau_{\text{rel}}) < t < \tau_{\text{bulk}}$, $p_{\text{reb}}(t) \sim t^{-3/2}$. An interesting regime is $\tau_{\text{mol}} < t < \tau_{\text{rel}}$ in the case that $\tau_{\text{rel}} > \tau_{\text{mol}}$ (panel B). It is seen that the simulation results suggest that $p_{\text{reb}}(t) \sim t^{-1/2}$ in this regime. This is predicted by the lower bound for $p_{\text{reb}}(t)$, Eq. S36, but not by the upper bound, Eq. S33 (see Fig. S2). This can be understood by noting that in this regime, $\tau_{\text{mol}} < t < \tau_{\text{rel}}$, the enzyme is mostly still inactive and the particle can thus diffuse away from the reactive sphere; while the lower bound of Eq. S36 captures this effect, the upper bound of Eq. S33 does not, since it is based on the inequality $p_2(\sigma, t - t' | r, 0) \leq p_2(\sigma, t - t' | \sigma, 0)$.

The effect of concentration. Fig. S4 shows the input-output relation as a function of concentration. Here, the concentrations of all components are increased by the same factor from the base-line values used in Fig. 5A of the main text. It is seen that both the particle-based model and the mean-field model predict that an increase in concentration induces bistability, although the concentration at which the bifurcation occurs is higher in the particle-based model.

Fig. S5 elucidates the origin of why an increase in concentration can induce bistability, both in the mean-field model and the particle-based model. Bistability arises when a substrate molecule that has been phosphorylated once, is more likely to be dephosphorylated again than to become fully phosphorylated (similarly, the probability that after a fully phosphorylated molecule has been dephosphorylated once becomes fully phosphorylated again, should be higher than that it becomes fully dephosphorylated). We therefore plot in Fig. S5 the probability that a substrate that has just been phosphorylated once, either binds the same kinase molecule as the one that just phosphorylated it (this is most likely due to a rebinding event), another kinase molecule (from the bulk), or a phosphatase molecule (from the bulk); the system is in a state where most substrate molecules are unphosphorylated. It is seen that the fraction of rebindings is fairly constant. This can be understood as follows: (1) the probability that a molecule returns to the origin before it loses memory

where it came from is independent of the concentration (see Fig. 2 of the main text)—only the memory-less returns from the bulk depend on concentration; (2) when a rebinding event happens, it happens very fast; as Fig. 2 of the main text shows, rebindings are dominated by events that occur on time scales of $t < 1$ ms. These time scales are so short, that the probability that an enzyme molecule from the bulk interferes with a rebinding event, is negligible, even up to concentrations of 100–1000 times the baseline value, i.e., 10 – 100 μM ; only above that concentration can molecules from the bulk effectively compete with those undergoing a rebinding trajectory, and will the probability that a dissociated molecule rebinds drop significantly. Up to a concentration of 10 – 100 μM , there is thus an essentially constant probability, independent of the concentration, that both sites of a substrate molecule are modified by the same enzyme molecule. Now bistability can arise when the antagonistic enzyme in the bulk wins the competition from the agonistic enzyme undergoing the rebinding event and the other agonistic enzymes in the bulk. Fig. S5 shows that when the concentration is increased, the competition between the kinase (the agonist) in the bulk and the phosphatase (antagonist) in the bulk changes in favor of the phosphatase. This is because the system is in a state where the substrate molecules are mostly unphosphorylated, and in this state the kinase molecules become increasingly sequestered by the unphosphorylated substrate molecules as the concentration is increased. This increases the probability that a molecule that has just been phosphorylated once, will bind a phosphatase (antagonist), which will drive it back towards the unphosphorylated state. Increasing the overall concentration thus changes the competition between the kinases and the phosphatases in the bulk in such a way that the driving force towards a state in which the substrate molecules are either fully unphosphorylated or fully phosphorylated, increases. In essence, increasing the concentration drives the system deeper into the bistable regime. This makes it possible to overcome the effect of rebindings, which tends to drive the system out of the bistable regime, as shown in Fig. 6 of the main text.

1. Takahashi K, Tănase-Nicola S, ten Wolde PR (2009) in preparation.
2. van Zon JS, ten Wolde PR (2005) Simulating biochemical networks at the particle level and in time and space: Green's function reaction dynamics. *Phys Rev Lett* 94:128103.
3. van Zon JS, ten Wolde PR (2005) Green's-function reaction dynamics: A particle-based approach for simulating biochemical networks in time and space. *J Chem Phys* 123:234910.
4. Morelli MJ, Tănase-Nicola S, Allen RJ, ten Wolde PR (2008) Reaction coordinates for the flipping of genetic switches. *Biophys J* 94:3413–3423.
5. Opplestrup T, Bulatov VV, Gilmer GH, Kalos MH, Sadigh B (2006) First-passage monte carlo algorithm: Diffusion without all the hops. *Phys Rev Lett* 97:230602.
6. Gillespie DT (1977) Exact stochastic simulation of coupled chemical reactions. *J Phys Chem* 81:2340.
7. Agmon N, Szabo A (1990) Theory of reversible diffusion-influenced reactions. *J Phys Chem* 92:5270–5284.

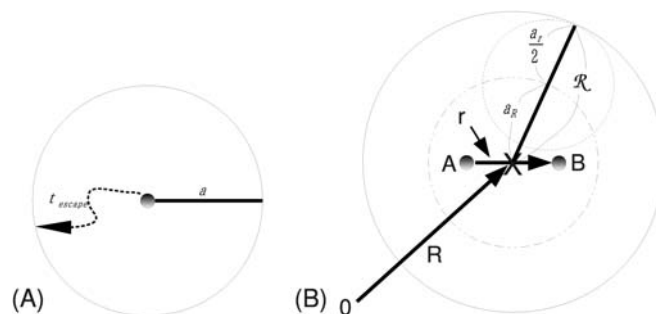


Fig. S1. Single and Pair objects. To solve the many-body problem exactly, protective domains are put around single particles (A) and pairs of particles (B). (A) The radius of the protective domain of a single particle is denoted by a . (B) To solve the reaction-diffusion problem of two particles that can react with each other and diffuse within a protective domain with radius \mathcal{R} , we construct two protective domains: one for the center-of-mass \mathbf{R} , with radius a_R , and one for the interparticle vector \mathbf{r} , with radius a_r . The radii a_R and a_r can be freely chosen, provided that when \mathbf{R} and \mathbf{r} would reach their maximum lengths, i.e., when $|\mathbf{R}| = a_R$ and $|\mathbf{r}| = a_r$, the particles A and B would remain within the protective domain. The latter means that a_R and a_r should satisfy the following two constraints: 1) $a_R + a_r D_A / (D_A + D_B) < \mathcal{R} - \sigma_A / 2$, which reflects that particle A should remain within the protective domain with radius \mathcal{R} ; 2) $a_R + a_r D_B / (D_A + D_B) < \mathcal{R} - \sigma_B / 2$, reflecting that B should remain within the protective domain with radius \mathcal{R} . Although a_R and a_r can be freely chosen provided that these constraints are met, an efficient choice is given by $a_R^2 / D_R^2 = (a_r - r_0)^2 / D_r^2$, meaning that the average time for \mathbf{R} to reach the boundary of its domain by free diffusion, equals that of \mathbf{r} . To illustrate the constraints, Panel B shows a scenario where \mathbf{R} and \mathbf{r} reach their maximum lengths; here, $D_A = D_B$.

